Journal of Radioanalytical and Nuclear Chemistry
https://doi.org/10.1007/s10967-024-09361-5

Development of low-temperature decontamination medium for decommissioning

Kateřina Čubová[1] · Mojmír Němec[1] · Tereza Šobová[1] · Barbora Drtinová[1]

Received: 7 October 2023 / Accepted: 4 January 2024

Abstract
Decommissioning is inevitable for each nuclear facility and, lately, it has become one of the most topical issues. Several decontamination methods have been successfully applied worldwide; however, variations in operating chemistry and/or different composition of the construction materials play a very important role and can cause unexpected problems. The experiments aim at dissolving the most resistant chemical present in corrosion layers, chromium (III) oxide, using redox chemistry and further test the found redox system on stainless steels and its model corrosion products. It was found out that persulfate solution in diluted sulfuric acid supported by Ag^+ ions can efficiently dissolve Cr_2O_3 and selected substrates at temperature as low as 50 °C.

Keywords Decontamination · Corrosion layer · Primary circuit · Persulfate · Decommissioning

Introduction

Closing the life cycle of nuclear power plant is a complex and long-term operation. Among the "hot" operations after transport of the used nuclear fuel, dismantling and fractionation of the primary circuit play the most significant roles. The decontamination of primary circuit focuses in the first step mainly on removal of inner corrosion layers containing activated corrosion products—and very often also immobilized fission products coming from microcracks in fuel cladding—adsorbed and/or incorporated during the NPP operation. During decommissioning, the methods can be more aggressive and should be much more efficient comparing to regular operational decontamination—the devices are not supposed to be used anymore for their initial purpose. The main goal is to minimize the activity before physical dismantling and cutting, thus minimizing amount of steel radioactive waste as well as protecting the personnel on site and minimizing their radiation dose.

Combinations of strong oxidative acid and complexing agent (e.g. HNO_3 and oxalic acid), mineral acid and strong oxidative agent (e.g. HBF_4 and $KMnO_4$) or strong mineral acid and redox system (e.g. H_2SO_4 and Ce^{3+}/Ce^{4+}) at elevated temperatures ranging 80–100 °C were applied in real decommissioning projects—e.g. MEDOC or DFD were used for decontamination of NPP primary circuits [1–11]. A key step in these decontamination methods is the dissolution of the various oxide compounds present in the corrosion layers on the inner surface of the stainless-steel pipes. Due to the composition of the construction materials and redox conditions during operation, mostly double oxides a spinel-like corrosion structures are the major compounds [12–14]. Their dissolution usually requires the oxidation of at least one of their building blocks, such as Fe(II) or Cr(III), to a higher valence state; very often, mainly in dissolving highly resistant chromium containing structures, trivalent chromium is targeted and oxidized to hexavalent. The resulting chromates are already well soluble. Similarly, it is possible to disrupt the spinel structure of magnetite by oxidation or reduction of its iron atoms.

Our research was focused on the development of a new chemical system suitable for decontamination of the primary circuit of a nuclear power plant with respect to construction materials, as well as operational and chemical history, with a priority focus on a VVER type plant, applicable especially in pre-disassembly decontamination in the decommissioning of a nuclear power plant.

✉ Kateřina Čubová
katerina.cubova@fjfi.cvut.cz

[1] Department of Nuclear Chemistry, Faculty of Nuclear Sciences and Physical Engineering, Czech Technical University, 115 19 Prague, Czech Republic

Published online: 06 February 2024

Experimental

Chemicals and materials

In the experiments, following chemicals were used: $AgNO_3$, $Na_2CrO_4 \cdot 4\ H_2O$, $Fe(NH_4)_2(SO_4)_2 \cdot 6\ H_2O$, Cr_2O_3, $Fe_2(SO_4)_3 \cdot 9\ H_2O$, and NH_4SCN (all p. a., Lachema); HNO_3 (63–65%, p.a., Lach-ner); H_2SO_4 (96%, p. a., Penta); Fe_3O_4 (≥ 97% Alfa-Aesar); $K_2S_2O_8$ (p. a., Roth). In addition to Fe_3O_4 and Cr_2O_3 used for basic dissolution testing, nickel–iron oxide Fe_2NiO_4 (≥ 98%, particle size < 50 nm, Aldrich) was chosen. Additional spinel materials were synthesized in ÚJV Řež, a.s. [15]. These materials were prepared as an analogue to spinel-like structures, which occur in the inner layers of corrosion layers in the primary circuits of nuclear power plants and represent an insoluble component. Elemental composition of the selected spinel-like materials preparation is summarized in Table 1 [15]. As the pristine steel material, stainless steel 08Ch18N10T was used as a representative of steels used in Czech VVER primary circuits.

Dissolution experiments

A set of experiments was performed to characterize the system selected and find out the influence of concentrations of components on the amount of dissolved metals. The oxidation and dissolution of common corrosion layer compounds was investigated in acidic environment of H_2SO_4 at various concentrations and temperatures.

In the procedures, the exact amount of substrate—chromium (III) oxide, magnetite or several spinel-like minerals synthetized [15] (see Table 1) was weighed into a test tube, respectively, acid solution of 40% H_2SO_4 was added, followed by immediate addition of $K_2S_2O_8$ solution as the oxidation agent, and $AgNO_3$ (0.1 $mol.L^{-1}$ solution) as catalyst. Tube was filled up to 10 mL with distilled water and carefully mixed. Resulting concentrations of $K_2S_2O_8$ in the range from 0.01 to 0.15 $mol.L^{-1}$; $AgNO_3$ catalyst (from 0 to 1.2 $mmol.L^{-1}$), and 5% H_2SO_4 were used. Samples ($V/m = 400\ mL.g^{-1}$) were then placed in a thermoblock, set to a temperature in the range 25–80 °C, and mixed thoroughly. For these batch experiments in vials, contact time was always set to 5 h. After a defined time, the samples were mixed again and finally centrifuged (5 min at 770 RCF). The concentrations of chromium, iron, and possibly nickel and manganese in the solution above the substrate were determined.

The kinetics of dissolution of magnetite and chromium oxide was investigated in order to know the time frame and the necessary retention of the solution in the flow arrangement. In the experiments Cr_2O_3, Fe_3O_4 and spinel material V17 were used. The experiments were performed according to the procedure described above and the optimum concentrations and temperature of the solution were used. In all cases, the residual concentration of persulfate in the solution was followed. The contact time was up to 24 or 48 h.

Table 1 Percentual composition of mixed materials (V11-V24) containing spinel-like minerals

Compound	Compound content in the mixed material [%]				
	V11	V13	V17	V20	V24
Cr_2O_3	26.7	30.0	–	–	11.7
Fe_2O_3	33.3	29.3	–	–	–
Fe_2NiO_4	40.0	40.7	–	–	–
$Cr_{0.4}Fe_{1.6}NiO_4$	–	–	–	–	73.6
$Cr_{1.6}Fe_{0.4}O_3$	–	–	–	–	14.8
$Cr_2Fe_2Ni_2O_3$	–	–	100	–	–
$Cr_{0.9}Fe_{2.8}Ni_{2.4}Mn_{1.6}O_3$	–	–	–	100	–

Measurement procedures

The persulfate concentration was determined spectrophotometrically immediately after sampling with Helios Epsilon spectrophotometer and PC software VISIONlite in version 2.1. Spectrophotometric method uses oxidation of Fe^{2+} to Fe^{3+} by the analysed sample in an acidic environment followed by ferric thiocyanate complex $Fe(SCN)_3$ formation in the solution. The detection limit at 450 nm ranges persulfate concentration down to $2 \cdot 10^{-4}$ $mol.L^{-1}$ [16, 17].

The content of Fe and Cr was determined with AAS in samples diluted up to 200 times to a volume of 5–15 mL. Standards were prepared from certified calibration solutions (Astasol, Analytika, s.r.o.) and acidified with 1% HNO_3. The calibration curve showed a good linear dependence in the whole range of tested concentrations—the sample matrix did not affect the linearity of the measurement. The measurement was performed on a Spectr AA—240 flame atomization instrument (Varian) with the evaluation in the PROMPT mode (maximum sample measurement time of 10 s). Iron was determined mostly in air acetylene flame in the range of 1–20 ppm at 248.3 nm with correction for non-specific absorption (N_2O acetylene flame was used during the optimization of the method), chromium in N_2O acetylene flame in the range of 1–10 ppm at 359.7 nm.

For each analytical method, standard uncertainties for the analysis and propagation of these uncertainties were determined using the error propagation law. For the spectrophotometric determination, an extended standard uncertainty of 5% was conservatively estimated, including both the inherent uncertainty of the measurement from the calibration curve as well as instrument error and pipetting error. Accuracy for AAS was verified using standards, which were

included in the measurements every 6 samples. If the deviation of the selected standard was greater, recalibration was performed. Each sample was measured twice.

For mixed Fe, Cr, Ni, Mn samples, ICP-OES in external laboratory was used, for all measured values an extended standard uncertainty of determination of 15%, corresponding to a 95% confidence interval were indicated. AAS measurements were taken with a maximum uncertainty of ± 5%.

Results and discussion

System optimization—temperature and concentration dependences

The selected chemical system was quantitatively characterized and the influence of the concentration of the individual components on the amount of dissolved chromium oxide was studied. First tests were carried out at the temperature of 80 °C (within the range of standard decontamination temperatures used) with concentrations of $K_2S_2O_8$ and $AgNO_3$ varied as shown in the Fig. 3. From these results, initial solution was selected as the basis of the decontamination method and further testing:

$$0.1\ \text{mol.L}^{-1}K_2S_2O_8,\ 0,8\ \text{mmol.L}^{-1}AgNO_3,\ 5\%\ H_2SO_4$$

Temperature dependence

Temperature dependence was studied on dissolution of Cr_2O_3 and Fe_3O_4 as model substrates according to procedure described above. The solubility was studied in the temperature range of 25–80 °C.

It can be seen (Fig. 1) that, the percentage of dissolved chromium increases with increasing temperature to a maximum between 45 and 53 °C, when more than 20% chromium passes into the solution. For temperatures higher than this maximum, the amount of dissolve chromium decreases gradually. Approximately 23% of the chromium is dissolved at the maximum. Comparable amount of chromium—approximately 7%—dissolves at room temperature (25 °C) and at 80 °C.

A similar set of experiments confirmed the dependence of Fe_3O_4 dissolving on temperature (Fig. 2). From the graph it is clear that the amount of dissolved iron increases over the entire range of measured temperatures. At 80 °C, over 70% of the iron was dissolved in 5 h, at 50 °C only about 26%. In this case, lowering the tempering temperature from 80 to 50 °C would reduce the percentage of dissolved iron by 44%. At 50 °C, the percentage of dissolved iron is comparable to the percentage of dissolved chromium.

The above described experiments have shown a significant influence of temperature on the efficiency of the process of dissolution. Despite relatively significant decrease in the dissolution efficiency of magnetite, the operating temperature was chosen to be 50 °C, which showed the highest efficiency for dissolving Cr_2O_3, because the solubility of this substance or its equivalent in the corrosion layer is supposed to be a limiting step in the developed decontamination process.

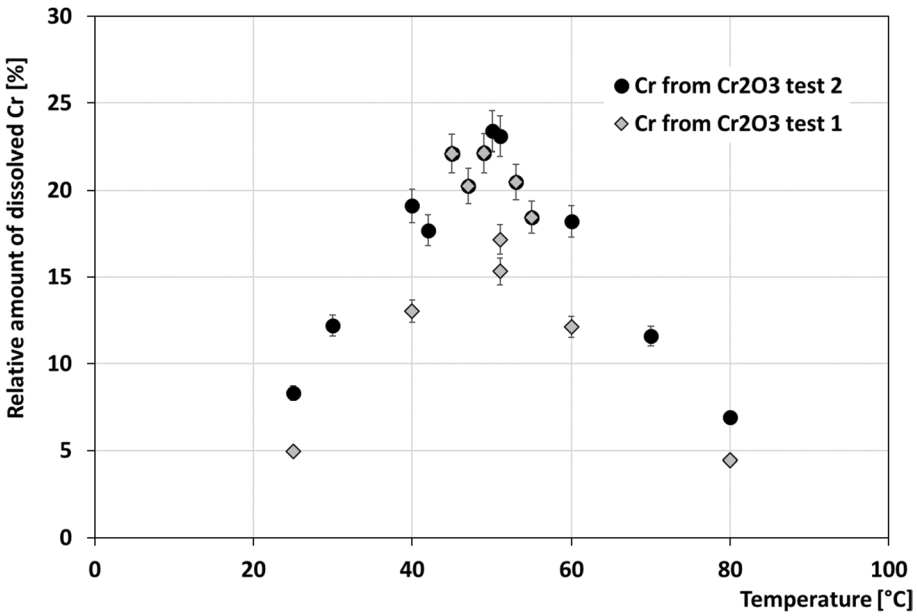

Fig. 1 Temperature dependence of Cr_2O_3 dissolution in (0.1 mol.L^{-1} $K_2S_2O_8$, 0.8 mmol.L^{-1} $AgNO_3$, 5% H_2SO_4), tempered for 5 h, V/m = 400 mL.g^{-1}

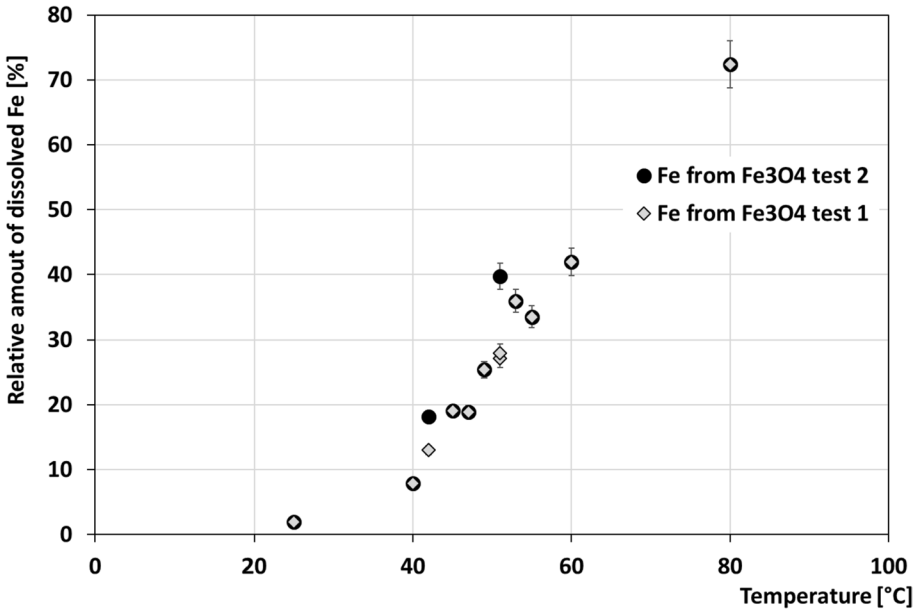

Fig. 2 Temperature dependence of Fe_3O_4 dissolution in (0.1 mol.L^{-1} $K_2S_2O_8$, 0.8 mmol.L^{-1} $AgNO_3$, 5% H_2SO_4), tempered for 5 h, V/m = 400 mL.g^{-1}

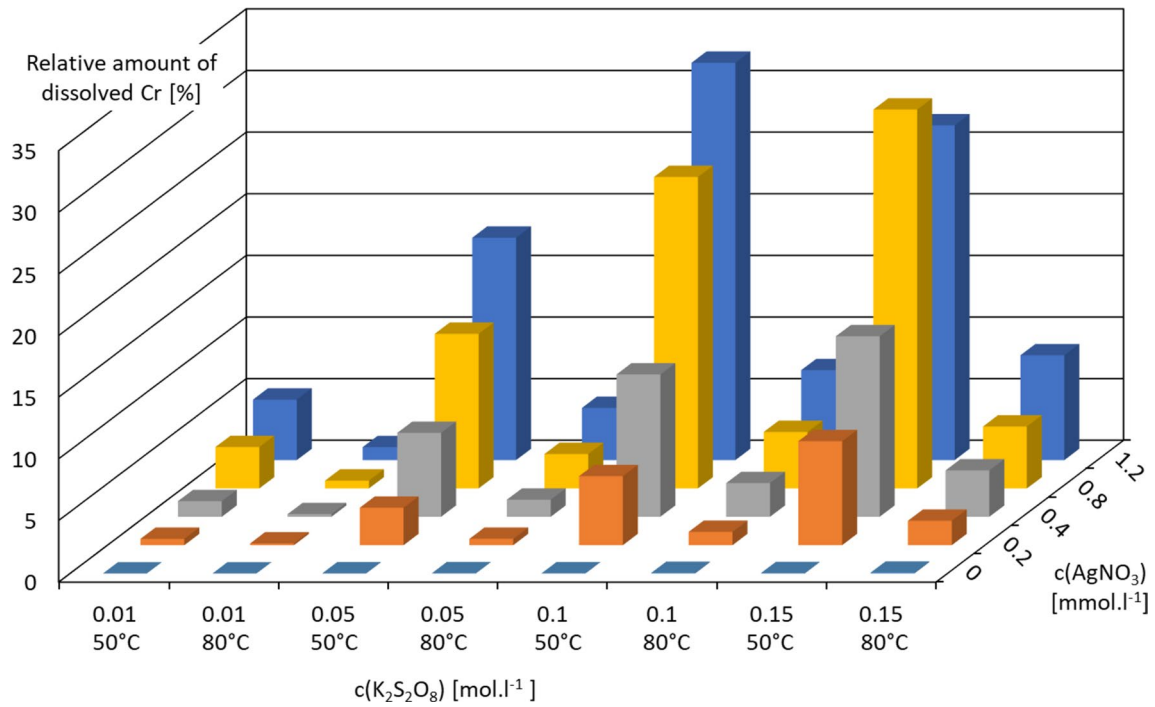

Fig. 3 Dissolution of Cr_2O_3 at 50 °C and 80 °C after 5 h in solutions with increasing concentrations of persulfate and added $AgNO_3$, V/m = 400 mL.g^{-1}

Verification of the effect of the decontamination solution composition at a temperature of 50 °C

After determining the temperature dependence of the dissolution of the model substrates, the effect of the concentrations of the individual components of the decontamination solution on its effectiveness at 50 °C was studied. In Figs. 3 and 4 below can be seen the quantities of dissolved iron resp. chromium depending on the concentration of $AgNO_3$ and $K_2S_2O_8$ in 5% H_2SO_4. The results led to the following conclusions:

- The solubility of Cr_2O_3 increases with increasing concentration of $K_2S_2O_8$ and $AgNO_3$, its solubility depends

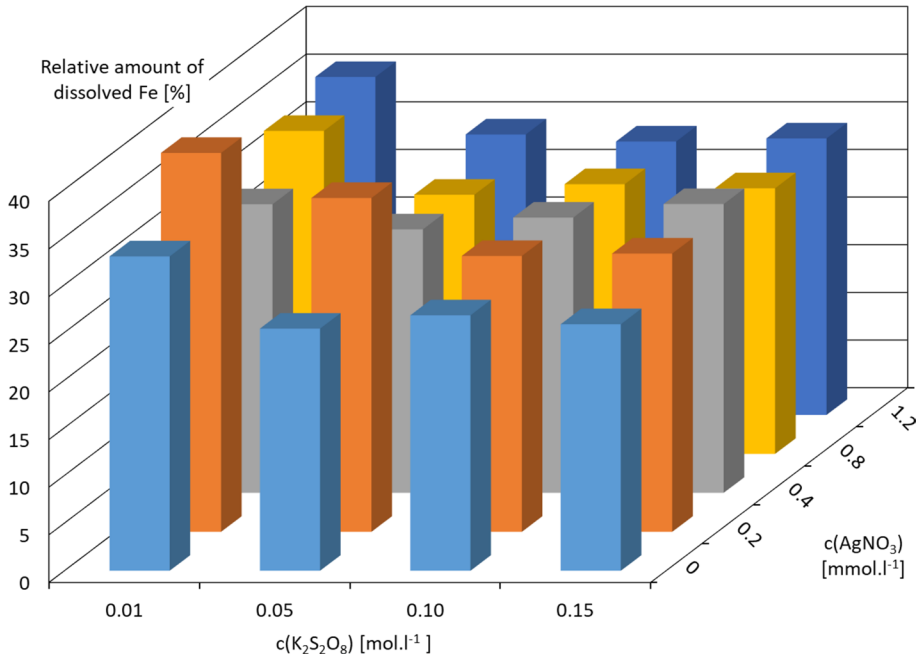

Fig. 4 Dissolution of Fe_3O_4 at 50 °C for 5 h in solutions with increasing concentrations of persulfate and added $AgNO_3$, V/m = 400 mL.g^{-1}

on the presence of both components. It can be seen that without the addition of $AgNO_3$, almost no Cr_2O_3 was dissolved (Fig. 3).

- The percentage of dissolved Cr is higher at 50 °C than at 80 °C in all the concentration intervals studied. In the media tested (0.1 mol.L^{-1} $K_2S_2O_8$, 0.8 mmol.L^{-1} $AgNO_3$, 5% H_2SO_4) the difference is up to 20%.
- The percentage of dissolved iron is much less dependent on the concentration of $K_2S_2O_8$ and $AgNO_3$ and the solubility of Fe in the whole range of tested concentrations is between 25 and 30%.

Dissolution of spinel-like materials

Experiments of dissolution of selected spinel-based material synthesized in ÚJV Řež, a.s. as more difficult to dissolve were performed—see Table 1 and [15]. Dissolution of these materials was carried out at the same conditions as the model materials. The solutions were heated for 5 h to 50 °C and 80 °C, respectively. The dissolution was evaluated by final Fe, Cr, Ni and Mn concentrations in the resulting solution, values are shown in Fig. 5.

From these results it can be seen that spinel-like materials dissolve mostly better at 50 °C and there is no preferential dissolution of any of the elements—the percentage of all dissolved elements is comparable. The only difference is material V20, but presence of manganese in its structure may introduce different dissolution mechanism—during dissolution the solution was pink coloured by produced permanganates, which could further and preferably at higher temperatures oxidize remaining bound chromium.

For further testing, material V17, for whom Cr, Fe and Ni were dissolved over 50%, was used to get better understanding of persulfate behaviour in the system and for more detailed investigation in determining of the dissolution rate.

Dissolution rate

Chromium oxide

As well as in the previous experiments, vials were mixed every 15 min, except in the case of experiments longer than 12 h. It was realized that the percentage of dissolved Cr is strongly dependent on such mixing at the beginning of the dissolution process, when it is increasing the yield of dissolved Cr for about 15%.

After 8 h, 28–35% of the chromium present was dissolved, similar value was achieved in the experiment of 42.5 h (Fig. 6). After 12 h the amount of persulfate decreased to 20% of the original value, after 24 h to 8%. It was also shown that at a persulfate concentration below 10% of the original value, no further dissolution of Cr_2O_3 occurred. Hence, the decrease of persulfate concentration in the system is caused not only by the reaction with Cr^{3+}—which is practically not running at this time—but also by the thermal decomposition of the persulfate.

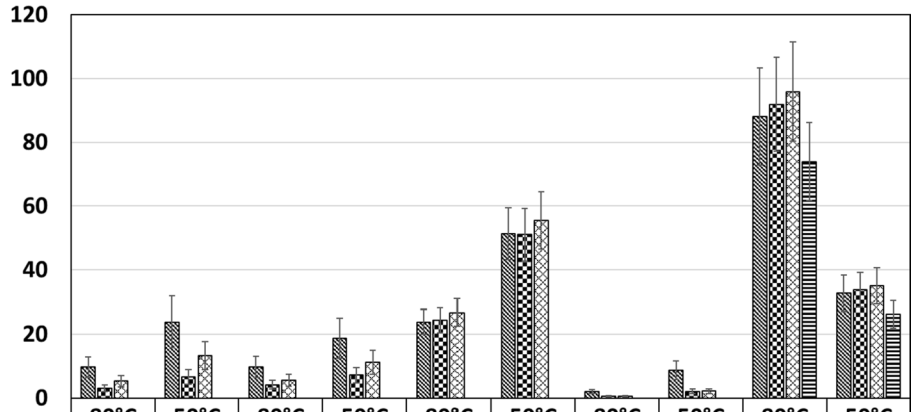

	80°C V11	50°C V11	80°C V13	50°C V13	80°C V17	50°C V17	80°C V24	50°C V24	80°C V20	50°C V20
Cr	9.64	23.83	9.77	18.63	23.8	51.3	1.95	8.73	88.0	32.7
Fe	3.13	6.60	4.19	7.18	24.3	51.0	0.61	2.08	91.9	33.7
Ni	5.32	13.30	5.53	11.16	26.7	55.5	0.59	2.15	95.8	35.0
Mn									73.9	26.2

Fig. 5 Percentage of dissolved metals from various spinel-like materials in (0.1 mol. L^{-1} $K_2S_2O_8$, 0.8 mmol.L^{-1} $AgNO_3$, 5% H_2SO_4), tempered for 5 h at 50 °C, resp. 80 °C, V/m = 400 mL.g^{-1}

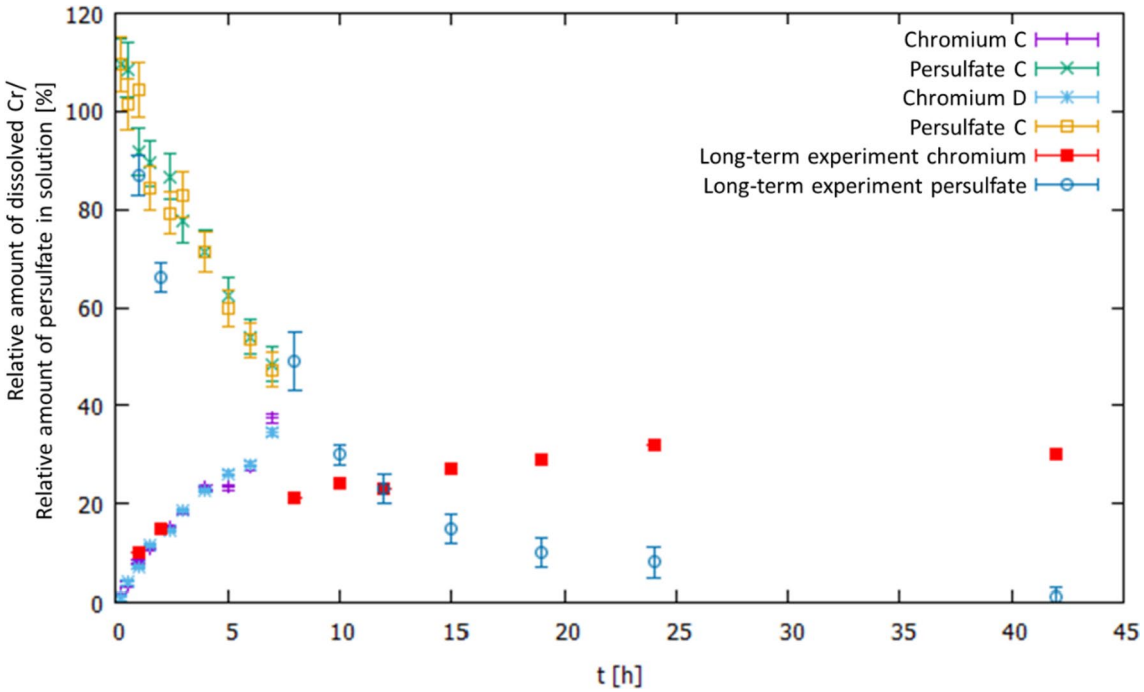

Fig. 6 Percentage of dissolved chromium and relative residual concentration of persulfate in solution when dissolving Cr_2O_3 in (0.1 mol.L^{-1} $K_2S_2O_8$, 0.8 mmol.L^{-1} $AgNO_3$, 5% H_2SO_4) at 50° C in long-term (42.5 h) and short-term experiment (7 h); C, D parallel samples, V/m = 400 mL.g^{-1}

Magnetite

Fe_3O_4 dissolves very well in the given system, even after the persulfate is spent. After 24 h almost 80% and after 42.5 h more than 97% of the iron was dissolved, while the concentration of persulfate was less than 10% resp. 1% at the end of the experiment (Fig. 7). It has been also found that the amount of dissolved iron depends much less on the mixing of the system than in the case of Cr_2O_3.

The dissolution kinetics of Fe_3O_4 and Cr_2O_3 showed that the persulfate is spent under the given conditions within 24 h. This time is sufficient to dissolve significant amounts of model substrates. In the case of magnetite, dissolution continues even after the exhaustion of persulfate up to 97%

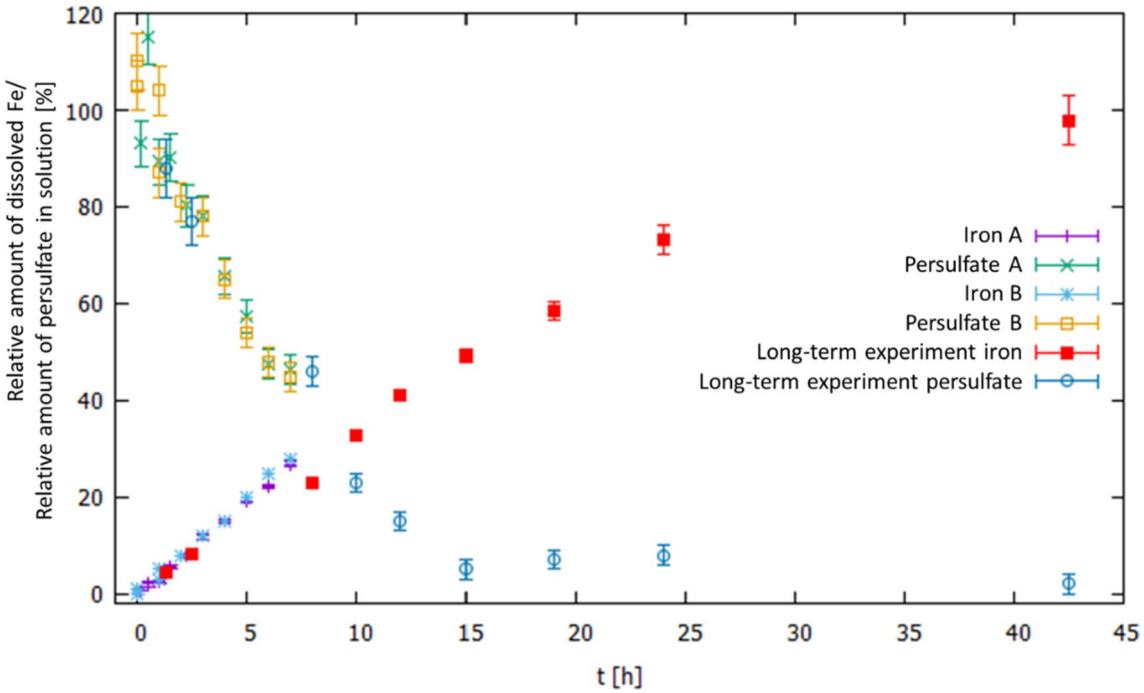

Fig. 7 Percentage of dissolved iron and relative residual concentration of persulfate in solution when dissolving Fe_3O_4 in (0.1 mol.L^{-1} $K_2S_2O_8$, 0.8 mmol.L^{-1} $AgNO_3$, 5% H_2SO_4) at 50° C in the long-term (42.5 h) and short-term experiment (7 h); A, B parallel samples, V/m = 400 mL.g^{-1}

in 42 h. For chromium oxide, the dissolution is terminated by a lack of oxidizing agent and about 30% of Cr was dissolved in 42 h.

Spinel materials

A spinel-based material marked V17 was selected for the kinetic experiment. The course of the experiment is shown in Fig. 8. It can be seen that iron, chromium and nickel dissolve equally. Both dependencies are growing in the whole range and do not reach the maximum. After eight hours, more than 55% of the iron, chromium and nickel are dissolved and about 35% of the persulfate from the original value still remains in the solution. Then, a long-term (42.5 h) experiment (Fig. 9) was performed in which the solutions were periodically mixed. It can be seen that the amount of dissolved metals increases in the whole range. After 24 h, approximately 60% of the iron, 80% of the chromium and 70% of the nickel were dissolved. After 24 h, there was practically no persulfate in the system.

Conclusions

The research was focused on finding a suitable chemical system that would effectively disturb and dissolve the corrosion layers formed on the inner surface of the primary circuit of the VVER type nuclear power plant (EDU and ETE) covered with 08Ch18N10T stainless austenitic steel. Problematic and hardly soluble components of the corrosion layers were selected—magnetite, chromium oxide and spinel materials with a higher chromium content. An important parameter both in terms of efficiency and chemistry of the whole process and economic is the temperature of the system. Especially in large volumes, heating or cooling of decontamination solution plays significant role in overall costs. Experiments have shown a significant effect of temperature on the dissolution efficiency of all materials tested.

It was found that optimised composition of the proposed decontamination solution is 0.1 mol.L^{-1} $K_2S_2O_8$ + 0.8 mmol.L^{-1} $AgNO_3$ + 5% H_2SO_4, well dissolving tested substrates at 50 °C. In the case of Cr_2O_3, when persulfate concentration fell below 10%, the dissolution stopped, but the magnetite dissolves even after all persulfate is spent. In all cases, the residual concentration of persulfate in the solution and its gradual decrease was observed.

The system developed was patented in 2021, patent No. 308870 "Recyclable medium for decontamination of primary circuit stainless steels during decommissioning of nuclear facilities" [18].

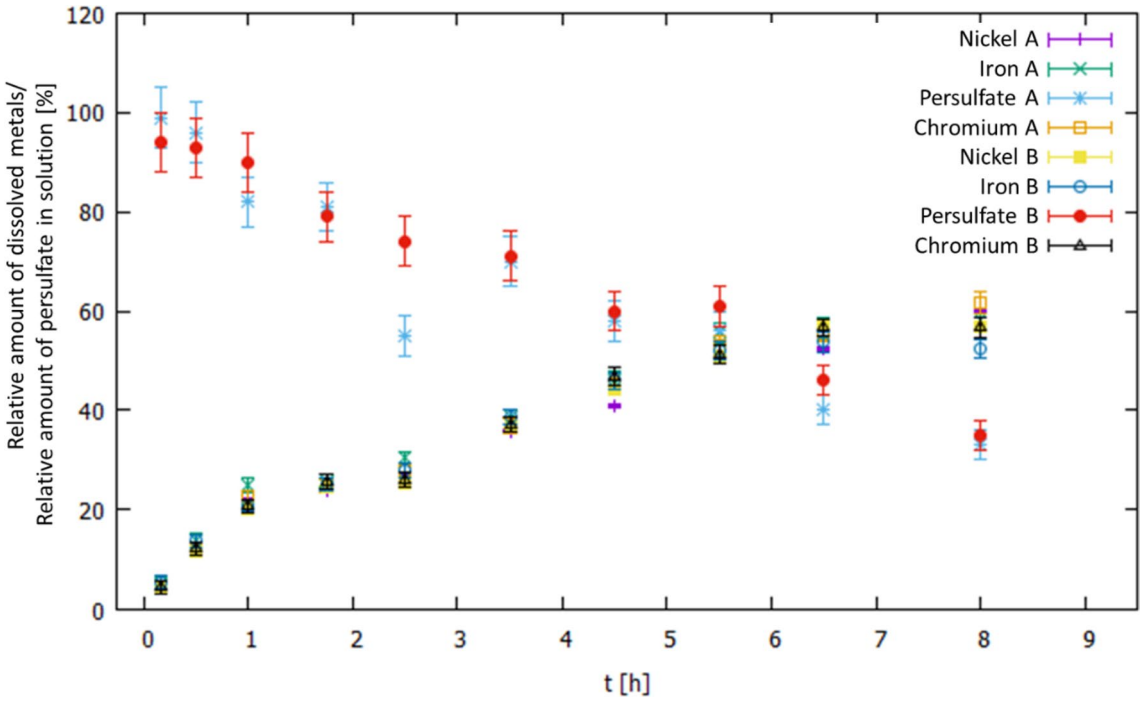

Fig. 8 The percentage of dissolved chromium, iron and nickel as a function of time and the percentage of persulfate remaining in the solution from the original value during dissolution of material V17 in (0,1 mol.L^{-1} M $K_2S_2O_8$, 0.8 mmol.L^{-1} $AgNO_3$, 5% H_2SO_4), tempered at 50 °C, V/m = 400 mL.g^{-1}

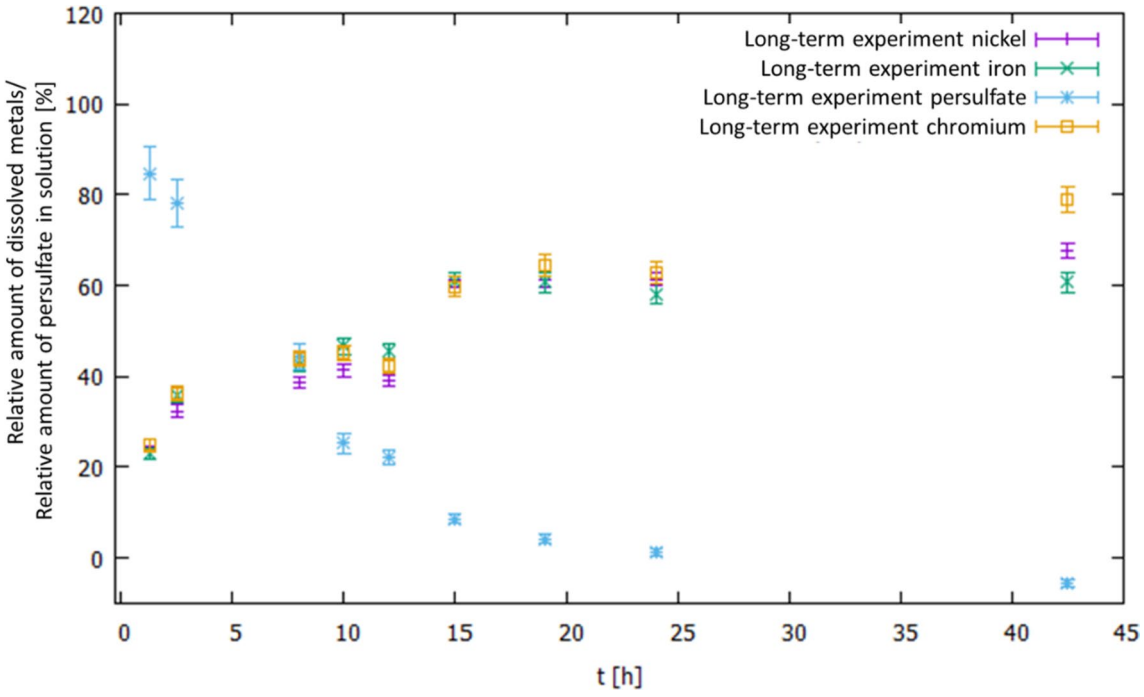

Fig. 9 Percentage of dissolved chromium, iron and nickel as a function of time and the percentage of persulfate remaining in the solution from the original value in (0,1 mol.L^{-1} M $K_2S_2O_8$, 0.8 mmol.L^{-1} $AgNO_3$, 5% H_2SO_4), tempered at 50 °C, V/m = 400 mL.g^{-1}

Acknowledgements This work was supported by Ministry of Trade and Industry of the Czech Republic under grant TRIO No: FV10023

and by Center for advanced applied science, project number CZ.02.1.01/0.0/0.0/16_019/0000778, supported by the Ministry of Education, Youth and Sports of the Czech Republic.

Funding Open access publishing supported by the National Technical Library in Prague.

References

1. Ponnet M, Klein M, Massaut V, Davain H, Aleton G (2003) Thorough chemical decontamination with the MEDOC process: batch treatment of dismantled pieces or loop treatment of large components such as the BR3 steam generator and pressurizer. In: WM 2003 conference. https://inis.iaea.org/search/search.aspx?orig_q=RN:35076640
2. Ponnet M, Klein M, Rahier A (2000) Chemical decontamination MEDOC using cerium IV and ozone. In: WM 2000 conference, Brussel, Belgium
3. Çetin Y, Acir A (2022) Decontamination applications in primary circuit equipment of nuclear power plants. Int J Energy Stud 7(2):195–216. https://doi.org/10.58559/ijes.1178889
4. Noynaert L, Bruggeman A, Rahier A, Cornelissen R (2001) WM 2001 conference (INIS-BE–0004). Belgian Nuclear Research Center SCK-CEN, Belgium
5. Decontamination techniqus used in decommissioning activities, a report by the NEA task group on decontamination. Nuclear Energy Agency (NEA) - Decontamination techniques used in decommissioning activities (oecd-nea.org)
6. Bradbury D, Elder G, Waite M (1996) Decontamination for decommissioning, EPRI DFD process. TR-106386. Final report. https://inis.iaea.org/search/searchsinglerecord.aspx?recordsFor=SingleRecord&RN=27066108
7. Bushart S, Wood CJ, Bradbury D, Elder G (2003) The EPRI DFDX chemical decontamination process. In: WM 2003 symposium, United States. https://inis.iaea.org/search/search.aspx?orig_q=RN:35076680
8. The EPRI DFDX process—final report: a process for the chemical decontamination of nuclear systems and components for disposal or refurbishment. EPRI, Palo Alto, CA (2006). https://www.epri.com/research/products/1013280
9. Development of the EPRI DFDX chemical decontamination process: a new process for the chemical decontamination of nuclear systems and components for disposal or refurbishment. Technical report. EPRI, Palo Alto, CA (2002). https://www.epri.com/research/products/000000000001003425
10. Decontamination handbook. EPRI, Palo Alto, CA. TR-112352 (1999). https://www.epri.com/research/TR-112352
11. Hahm I, Kim D, Ryu HJ, Choi S (2023) A multi-criteria decision-making process for selecting decontamination methods for radioactively contaminated metal components. Nucl Eng Technol 55(1):52–62. https://doi.org/10.1016/j.net.2022.09.012
12. Varga K, Baradlai P, Hirschberg G, Németh Z, Oravetz D, Schunk J, Tilky P (2001) Corrosion behaviour of stainless steel surfaces formed upon chemical decontamination. Electrochim Acta 46(24):3783–3790
13. Szabó A, Varga K, Németh Z, Radó K, Oravetz D, Makó KÉ et al (2006) Effect of a chemical decontamination procedure on the corrosion state of the heat exchanger tubes of steam generators. Corros Sci 48(9):2727–2749
14. Grygar T, Zmitko M (2002) Corrosion products behaviour under VVER primary coolant conditions. https://inis-iaea.org/collection/NCLCollectionStore/_Public/34/057/34057641.pdf (iaea.org)
15. Kašpar M (2018) Spinel preparation data. ÚJV Řež a. s https://kerntechnik.com/wp-content/uploads/2023/06/Proceedings.zip
16. Huang K, Couttenye RA, Hoag GE (2002) Kinetics of heat-assisted persulfate oxidation of methyl tert-butyl ether (MTBE). Chemosphere 49(4):413–420. https://doi.org/10.1016/S0045-6535(02)00330-2
17. Waclawek S, Lutze HV, Grübel K, Padil VT, Cernik M, Dionysou DD (2017) Chemistry of persulfates in water and wastewater treatment: a review. Chem Eng J 330:44–62
18. Patent: CTU in Prague, Praha 6, Dejvice, CZ; ÚJV Řež, a.s., Husinec, Řež, CZ. CHEMCOMEX, a.s., Praha 5, Zbraslav, CZ. The method of decontamination of the internal surfaces of the primary circuit of the nuclear power plant and the decontamination solution. Inventors: Němec M, Čubová K, et al. Czech Republic. Patent CZ308870, 15 July 2021